

Towards large-scale, automated, accurate detection of CCTV camera objects using computer vision

Applications and implications for privacy, safety, and cybersecurity

(Preprint)

Hannu Turtiainen [†]
University of Jyväskylä

Jyväskylä, Finland
hannu.ht.turtiainen@student.jyu.fi

Andrei Costin [⊗]
University of Jyväskylä
Jyväskylä, Finland
ancostin@jyu.fi

Timo Hämäläinen
University of Jyväskylä
Jyväskylä, Finland
timoh@jyu.fi

Tuomo Lahtinen
University of Jyväskylä
Jyväskylä, Finland
tuomo.t.lahtinen@student.jyu.fi

Abstract—While the first CCTV camera was developed almost a century ago back in 1927, currently it is assumed as granted there are about 770 millions CCTV cameras around the globe, and their number is casually predicted to surpass 1 billion in 2021. Similarly to the first prototypes from 1927, at present the main promoted benefits for using and deploying CCTV cameras are the physical security, safety, and prophylactics of crime. At the same time the increasing, widespread, unwarranted, and unaccountable use of CCTV cameras globally raises privacy risks and concerns for the last several decades. Recent technological advances implemented in CCTV cameras such as AI-based facial recognition and IoT connectivity only fuel further these concerns raised by privacy-minded persons.

However, many of the debates, reports, and policies are based on assumptions and numbers that are neither necessarily factually accurate nor are based on sound methodologies. For example, at present there is no accurate and global understanding of how many CCTV cameras are deployed and in use, where are those cameras located, who owns or operates those cameras, etc. In addition, there are no proper (i.e., sound, accurate, advanced) tools that can help us achieve such counting, localization, and other information gathering. Therefore we cannot objectively evaluate the state of the global video surveillance, its negative effects on privacy, and its positive impact on safety. Currently employed methods involve manual counting and positioning, using inflated “sales figures” and outdated/sparse/unvetted datasets, and applying unjustified extrapolations. Obviously such techniques are inaccurate, do not scale, do not provide a clear picture, and do not provide a scientific base for reasoning, debate, and policy-making. Therefore, new methods and tools must be developed in order to detect, count, and localize the CCTV cameras. Those methods must be scalable, accurate, based on sound scientific approaches, and easily applicable in real-life.

To close this gap, with this paper we introduce the first and only computer vision MS COCO-compatible models that are able to accurately detect CCTV and video surveillance cameras in images and video frames. To this end, our state-of-the-art detector was built using 3401 images that were manually reviewed and annotated, and achieves an accuracy between 91,1% – 95,6%. Moreover, we build and evaluate multiple models, present a comprehensive comparison of their performance, and outline core challenges associated with such research. We also present possible privacy-, safety-, and security-related practical applications of our core work. Last but not least, we release as open-data and

open-source relevant data and code that can be used to validate and further extend our work.

Index Terms—CCTV, cameras, video surveillance, privacy, safety, computer vision, object detection, machine learning, open-source, open-data, datasets

I. INTRODUCTION

CCTV and video surveillance cameras represent nowadays some of the most ubiquitous technology, and it is almost impossible to live a day without getting into the field of view of at least one CCTV camera [2]. At present, CCTV cameras are an integral part of any infrastructure (e.g., cities, buildings, streets, businesses), and it is expected that by 2021 there will be more than 1 billion CCTV cameras globally [3]. Meanwhile, the earliest known CCTV-precursor goes back as early as 1927 when the Soviet inventor Leon Theremin installed the first real-world usable prototypes of then-called *distance vision* along the Kremlin premises [4]. It was a mechanically-operated device that transmitted a few hundred image-lines which allowed however the user operator to distinguish and recognize faces.

When it comes to cybersecurity, CCTV cameras are already known to be the subject of numerous cyberattacks [5], and they were also the main culprit behind the now legendary and massive attack by the Mirai IoT botnet [6]. At the same time, it is long and well known that CCTV cameras raise concerns and pose risks related to privacy [7]–[11]. However, it is very hard (if not impossible) at present to accurately and objectively assess and address the privacy risks and implications of certain claims or facts. For example, in order to assess how serious is a privacy risk of a certain CCTV installation, we need to identify and count precisely the CCTV cameras, and we need to know exactly where the cameras are located along with their other characteristics such as field of view, zoom levels, and other built-in features (e.g., face recognition, Infra-Red (IR), Pan-Tilt-Zoom (PTZ)).

Unfortunately, most of the current data publicly available about CCTV cameras statistics and characteristics, both at global and local levels, can be considered *completely unre-*

[†] This paper is based on author’s MSc thesis [1].

[⊗] Corresponding and original idea’s author.

liable. As follows, we provide several such examples that demonstrate the unsound methodologies and discrepancy in data. In one instance, UK had until 2014 three different major estimations about the number of CCTV cameras – 1.8 mil. [12], 4.2 mil. [13], and 5.9 mil. [14]. To add insult to the injury, despite the rampant increase of CCTV and video surveillance globally, these numbers were not updated ever since, and are referenced in 2019–2020 as “current” by various reports and media outlets. In another instance, the estimates for global number of CCTV cameras vary between 25 mil. [15] and 770 mil. [3] – a whopping 25x discrepancy. In yet another instance, UK finds that on average a person enters a CCTV camera view 300 times a day [15]. A similar study in US puts that number at 50+ times a day, despite the more worrying fact that the average US respondent *assumed it was 4 cameras or less* [16] – at least a 10x lower presumed privacy risk and exposure than in reality. At the same time, a recent journalist experiment in NYC (US) by Pasley [2] found he encountered CCTV cameras face-to-face at least 49 times, and that is *just counting a single trip to the workplace*. Finally, there are also discrepancies related to number of cameras per 1000 persons [12], [14], [17].

A quick check reveals that such discrepancies may have several root-causes. In some cases, it is the use of unsound and low-tech methods, such as visually counting CCTV cameras on a *single main shopping street in London*, and then extrapolating (by some unvetted model) the numbers to the entire country [13]. In other cases, it is the heavy use of sales and marketing data [3], which by our experience very often is unrepresentative, highly approximated, and over-estimated. Even if we would assume the rightfulness of counting data provided by such unscientific methods, they cannot however provide the privacy-critical information about any camera, namely its location, characteristics (e.g., field of view, zoom), and spatial coverage.

There are many ways to mitigate the privacy risks posed by CCTV cameras (including their additional features such as face recognition). One possible way is to use artistic (but perhaps unpractical and low-tech) methods such as specially-designed transparent plastic masks [18] or face painting (i.e., “adversarial computer vision” attack) [19]. However, these methods could be easily defeated as the advances in computer vision and face recognition are extremely fast, allowing correct identification through face recognition even when the subjects wear respiratory masks [20].

Another possible way is to develop, provide and use appropriate high-tech tools against the invasion of privacy by CCTV cameras. Examples of such tools include CCTV-aware route planning and navigation, and real-time early warning system when mobile and embedded devices that are video-input equipped (e.g., wearable devices, smartphones, drones) enter areas under the potential field of view of CCTV cameras. Therefore, such tools require trustworthy object detection and counting, and accurate mapping and localization. In this context, computer vision is a proven method that excellently performs for object detection and counting [21], as well as for

mapping and localization [22], [23].

In this paper we try to close the existing fundamental research and technology gap, and to address the strong and imminent need in such tools. To this end, we developed the first and state-of-the-art CCTV camera object detector using latest computer vision techniques. We also prototype and discuss CCTV-aware privacy-oriented applications that build atop of our detectors. During the experiments on real-world data, our system achieved an accuracy between 91,1% – 95,6%, which is comparable to Google’s original automatic system for large-scale privacy protection of human faces and car license plates in Google Street View [24].

A. Contributions

- We are the first to research, implement and evaluate the state-of-the-art Computer Vision (CV) models to detect *CCTV camera objects* in images and video frames.
- We release as *open data* the models and datasets necessary to validate our results and to further expand the datasets and the research field. To our knowledge, these are the first, the largest, and the best-performing datasets and models to be publicly released for solving the stated problems.
- We are first to introduce and motivate a handful of *CCTV-aware* applications for both privacy and safety scenarios as relevant for modern digitized lifestyle.
- We release the relevant artefacts (e.g., code, datasets, trained models, and documentation) at: <https://github.com/Fuziih> and <https://etsin.fairdata.fi/dataset/d2d2d6e2-0b5c-46e0-8833-53d8a24838a0> (urn:nbn:fi:att:258ce5ad-9501-46b9-a707-c1f59689ee10).

B. Paper organization

The rest of this paper is organized as follows. In Section II we overview the related work. We detail our methodology and describe our experimental setup in Section III. Then, in Section IV we present our results and main findings. In Section V we discuss the caveats, possible applications, and future work. Finally, we conclude with Section VI.

II. RELATED WORK AND STATE OF THE ART

A. Object Detection Systems

1) *Detectron2* [25]: is “Facebook AI Research (FAIR)’s next generation software system that implements state-of-the-art object detection algorithms”. It is a complete rewrite of the open source object detection platform Detectron [26], and originated from FAIR’s successful maskrcnn-benchmark project [27]. FAIR suggests that the modularity of the framework grants the users flexibility and extensibility to train and use state-of-the-art object detection algorithms with various system configurations ranging from single GPU PCs to multi-GPU clusters [25].

2) *CenterMask2* [28]: is an upgraded implementation of CenterMask [29] for the Detectron2 [25] framework. CenterMask (CM) and CenterMask2 (CM2) are segmentation-based architectures built upon the Fully Convolutional One-Stage Object (FCOS) architecture [30]. In essence, CenterMask is a

three-part architecture consisting of VoVNet2 [31] backbone (for feature extraction), detection head (lifted from FCOS), and the mask head.

At its core, CenterMask/CenterMask2 predicts the object centerpoint locations from an image, and estimates the key-points of the object. Then feature representation at the center point is lifted, and it forms the local shape of an object. Local shape is, in essence, a coarse mask over the object that separates the detected object from everything else close by. During this operation, the backbone assembles a global saliency map of the image at pixel level. This map separates the foreground from the background. Finally, the local shapes and global saliency maps are assembled to create the final instance maps [29].

3) *TridentNet* [32]: approaches the object detection challenge through the problem of scale variation of the detected objects. Its authors propose scale-aware *Trident Networks* concept, which aims to create scale-specific activation maps. The network uses multi-branch architecture with equal transformation parameters, but different kernel receptive fields. In addition, a scale-aware training process specializes every branch with specific scale of objects [32].

TridentNet uses its own approach to extract features of different scale. Using dilated convolutions [33], different branches share the network structure producing comparable features but having different scales due to the receptive field variance. Dilated convolution is then applied to the branches with varying dilation rates. This means that convolutions are performed at sampled locations, which are chosen sparsely. In turn, this increases the size of the receptive field. The receptive fields are therefore accommodated to different scales of objects. This multi-branch regime could introduce many new parameters as the branch count increases. TridentNet however, introduces weight sharing to the process. As the branches are identical, except the receptive field dilation rate, weight sharing ideally fits the purpose. Therefore, same parameters are trained for different object scales. To combat scale mismatch caused by the predefined dilation rates in the multi-branch architecture, Li et al. [32] propose scale-aware training, which selects correct ranges in the branches for each pair of $\langle \text{proposal}, \text{ground truth} \rangle$.

4) *ATSS* [34]: starts from the premise that a key difference between anchor and anchor-free detectors is how they characterize their positive and negative samples. The Adaptive Training Sample Selection (ATSS) uses the object’s statistical characteristics to select the sample accordingly. With ATSS, Zhang et al. [34] leveled the playing field between the prominent detectors – anchor-based RetinaNet [35] and anchor-free FCOS [30]. They achieved this by setting key configurations similarly, therefore introducing almost similar performance (37% vs. 37.8% in MS COCO [36] *minival subset*). With the introduction of these similar configurations, the authors were able to determine that the differences between the two detectors boiled down to how they determine two core things – the positive and negative samples (classification) and the starting point for the bounding boxes (regression). The authors allow

only one anchor box per location when using RetinaNet [35] as this procedure is close to the methodology of FCOS [30]. Otherwise, by default RetinaNet [35] pushes nine anchors per location. With further testing, ATSS authors concluded that when the sample selection of the detectors is similar, the effects of the bounding box regression starting point on performance of FCOS is negligible. Therefore, it makes the manner of classification an irrelevant difference between the detectors. ATSS tests conclude that training sample selection is an essential aspect of the training performance of any detector, and therefore an interesting avenue for research [34].

B. Object Detection Datasets

Lin et al. [36] proposed a novel dataset for general object detection called Microsoft’s Common Objects in COntext (COCO, or MS COCO). The most recent (2017) update of MS COCO has a fully annotated training dataset containing 118000 images and a 5000 image validation dataset. In addition, a 41000 image testing dataset is also available. There are more than 80 different classes for state-of-the-art object detector testing with the MS COCO [37], including pedestrians, traffic lights, cars, and even teddy-bears. However, it does not contain object detection models for CCTV cameras, though they are currently an indispensable part of any street and city infrastructure such as traffic lights and road signs.

PASCAL Visual Object Classes (VOC) [38] project ran object detection challenges between 2005–2012 [39]. For the 2012 object detection challenge, PASCAL VOC dataset labeled 20 classes with both training and validation datasets, and provided more than 11000 images totaling over 27000 instances [40]. The dataset contained several similar classes to increase difficulty [41].

ImageNet Large Scale Visual Recognition Challenge (ILSVRC) [42] is an ongoing annual object category classification and detection challenge that has been run since 2010. Russakovsky et al. [42] envisioned ILSVRC to follow PASCAL VOC [38] footsteps in providing a challenging dataset and hosting competitions. ImageNet provides about 1.2 million images for training and around 150000 images for validation and testing. ImageNet has 1000 classification labels, of which 200 were originally chosen for object detection challenges [42].

Open Images Dataset V6 contains over 9 million annotated images for a total of more than 15 million bounding boxes covering about 600 object classes [43]. The Open Images project holds the annual Robust Vision Challenges, and their goal of is to further improve the development of computer vision systems [44].

In this context, our work is novel and perfectly extends the state of the art by contributing both the methods (e.g., scripts), as well as annotated data and trained models necessary for object detection of two classes of CCTV cameras (directed and round – see Section III-A).

C. Computer vision / object detection on street-level imagery

There are numerous companies and projects capturing and serving street-level imagery such as Google Street View,

EveryScape, Mapjack, Microsoft StreetSide, Yandex Street Panoramas, OpenStreetCam, Mappillary. Such imagery allows much richer online and offline experiences boosted by technological advances in Computer Vision (CV), Machine Learning (ML), Natural Language Processing (NLP) with text mining, Virtual/Augmented/eXtended Reality (VR, AR, XR). Overall, capturing street-level imagery presents both tremendous challenges and opportunities [45].

Paiva [46] used “*computer vision to infer urban indicators on google street view*”. Wojna et al. [47] presented a method for “*extraction of structured information from street view imagery*”. Hara et al. [48]–[51] used “*google street view using crowdsourcing, computer vision, and machine learning*” for an extensive set of detections and challenges related to street-level accessibility for persons with special needs. Frome et al. [24] presented methods for large-scale privacy protection in Google Street View imagery. Using their fully automatic system the authors were “*able to sufficiently blur more than 89% of faces and 94–96% of license plates in evaluation sets sampled from Google Street View imagery*”. Related to the accurate mapping of an image based on street-level imagery, Zamir and Shah [52] introduced methods for image localization using Google Street View with an accuracy comparable to GPS-based technology.

However, none of the existing works attempted to perform detection and accurate location mapping of CCTV camera objects from street-level imagery. In this context, our work is the first to achieve this and perfectly extends the state of the art by accurately detecting CCTV cameras on both street-level and other imagery (both geo-tagged and not).

D. Face recognition, privacy and CCTV/IP cameras

Face recognition is a very hot topic, has been a prolific areas of research, and there is an immense body of works [53]–[59]. At the same time, (near) real-time face detection, tracking, and recognition is one of the core applications of CCTV cameras which is increasingly gaining traction. Several papers have been released on the subject of facial detection and recognition in real-time recordings such as the ones in CCTV setups. Halawa et al. [60] recently showed how the *Faster R-CNN* [61] algorithm is used with face detection in CCTV systems. Once a face is detected from a recording, an image can be stored for facial recognition by a slower algorithm, which can extract features from it. Bah and Ming [62] presented their facial recognition algorithm. Their method includes prepossessing the images to better capture facial features and then implementing their own Local Binary Pattern (LBP) algorithm [56]. Mileva and Burton [63] demonstrated the use of facial recognition in a noisy real-life environment such as in CCTV camera footage. The authors conclude that facial recognition from CCTV footage is certainly an arduous task and prone to errors [63]. Worse, erroneous face recognition results may lead to arrests of innocent persons, such as the infamous case of Steve Talley who got arrested twice in two separate bank robbery cases and both times the arrests were found to be wrong [64].

However, large CCTV networks may provide unaccountable access to their video streams, turning them into tools of mass illegal surveillance. For example, a recent journalist investigation in Russia demonstrated that it is extremely easy to acquire access to high-quality video feeds of almost 200k state-operated CCTV cameras within Moscow’s digital surveillance network [65]. Additionally, the researchers were able for a fee to get access to the “*face search*” feature, where the requestor provides a photo containing a “reference face”. Then, the facial recognition sub-system of the CCTV network provides back an extensive list of exact geo-locations (and other meta information) where similarly matching faces were previously seen within the CCTV network. The access to video feeds and to the “*face search*” feature is allegedly sold for a very low fee on underground and specialized forums by unscrupulous law enforcement officers (i.e., a particular instance of the *insider threat* [66], [67]).

In this context, our research, through the automated CCTV camera detection (having as immediate goal accurate mapping of camera geo-locations and characteristics) aims to provide users with tools for a more democratic use of technology where privacy controls are on the users’ side. For example, such tools may help the users to make an informed and real-time decision whether they want to be (or not!) in an area within the field of view of CCTV cameras.

E. Cybersecurity and CCTV/IP cameras

Recent research demonstrated that the state of cybersecurity for IoT devices (including DVRs and CCTV/IP cameras) and their firmware is very bad [68]–[70]. Back in 2013, independently and almost simultaneously Heffner [71], Costin [72], Shekhan and Harutyunyan [73] researched and presented about vulnerabilities, exploits and cybersecurity dangers related to vulnerable and exposed CCTV/IP/surveillance cameras. In particular, [72] proposed several hypotheses related to (in)security of CCTV/IP cameras, which were later extended and systematized in [5], and we summarize some of them below. One research observation was the dangerous potential of easy “harvesting” of vulnerable cameras into botnets. Another hypothesis was the realistic possibility of massive unauthorized access to video feeds for various illegal or unethical purposes, including blackmailing or extortion ¹ as well as “person search” driven for example by missing persons alerts, “head bounties” or other surveillance motives ². Unsurprisingly, in 2013–2014 reports started to surface about the infamous (and supposedly Russian-operated) Insecam project [74], [75], which at its peak featured between 100–200k video feeds from vulnerable/insecure CCTV/IP cameras connected to the internet. Moreover, in late 2016 news broke about the infamous and devastating Mirai IoT botnet [6], [76]. It featured the largest known DDoS attacks to date of over 1 TB/s, employed at peak about 600k devices, took down major parts of the

¹Proposed also in 2017 by Antonakakis et al. [6].

²Discovered in late 2019 to be happening in Russia [65] – see more in Section II-D



Fig. 1. Examples of *directed camera* class (images CC0 by unsplash.com).

internet, and mostly consisted of hacked CCTV/IP cameras and CCTV/DVR surveillance systems.

While this work does not explicitly address the cybersecurity of CCTV cameras, one possible offensive scenario to consider is presented in Section V-C.

III. METHODOLOGY AND EXPERIMENTAL SETUP

As with any Computer Vision (CV) object detector, we followed a two-phase approach. First, we trained multiple models for object detection with our “training dataset”. In order to train the CV object detectors, we split the phase into four parts – dataset gathering (Section III-A), image annotation (Section III-B), environment setup (Section III-C), and model training (Section III-D). Then, we evaluated each trained model against a “test dataset” which was kept the same for all the models at any given evaluation point (see Section IV).

A. Dataset gathering

When we started to gather the dataset, we made a practical decision that we want to be able to classify the cameras into at least two distinct classes based on their shape – *directed cameras* and *round cameras*. Having this information allows us in the future work to model more accurately their field of view coverage in 3D, therefore allowing to decide whether a particular point in space (e.g., sidewalk, street, street corner) provides or not privacy to a person.

Directed cameras include box- and bullet-shaped cameras (see Figure 1), and we assume such cameras record a limited field of view specifically in the direction they are pointed to. Some of them may be motorized (e.g., via Pan-Tilt-Zoom (PTZ) hardware and protocols) and therefore be able to have a mobile field of view (in theory up to 360°). However, it is challenging (if not impossible) to detect PTZ with computer vision on static (and low resolution) images. Therefore, to simplify a bit our experiments and future geo-mapping modeling, we assume that such cameras are static, cover the particular direction they are pointed to, and have limited vertical and horizontal fields of view.



Fig. 2. Examples of *round camera* class (images CC0 by unsplash.com).

Round cameras include dome- and sphere-shaped cameras (see Figure 2), and we assume such cameras potentially record a 360° field of view. Even though some dome- and sphere-shaped cameras host inside a static and directed camera sensor, most of the times it is challenging to know that because of the reflective glass. Therefore, to simplify a bit our experiments and future geo-mapping modeling, we assume that such cameras record a 360° field of view.

1) *Training and validation datasets:* Our training dataset contains 3401 images for a total of 2244 directed class instances and 1742 round class instances. Our validation dataset contains 528 images for a total of 348 directed class instances and 269 round class instances, marking about 15,5% split between training and validation datasets. For the datasets, we used the MS COCO format as this made it easy to use several object detection architectures out of the box (see Section III-D), and it also allowed instance segmentation detection thanks to the polygon annotation possibility.

2) *Testing dataset:* For evaluation purposes (see Section IV), we gathered a separate test dataset. The test dataset contained only street-level imagery sources such as OpenStreetCam [77] and Google Street View [78]. The test dataset is intended to serve as an indicator how well our trained models will work as CCTV camera detectors specifically for street-level imagery sources since such sources are the primary use case proposed for future work. Our test dataset contains 186 images for a total of 126 instances of *directed cameras* class and 105 instances of the *round cameras* class.

B. Image annotation

Since we use supervised training at this stage, we have to label and annotate the images in our datasets. To annotate the images, we used Wada’s Labelme tool [79]. Labelme is heavily inspired from the work by Russell et al. [80] who created LabelMe, which is a web-based image annotation and labeling tool. Wada’s Labelme [79] allows annotation with polygon segments that can be used in object segmentation architectures such as Mask-RCNN [81] and CenterMask [29]. When using object segmentation, the outlines of the objects can be identified more precisely instead of a mere bounding box around the

object of interest. Also, Wada’s Labelme outputs individual JSON files for each annotated image, and includes Python scripts to embed the data as a single annotation file in MS COCO format [79]. We annotated the final versions of our datasets (i.e., training, validation, testing) with polygon shapes, and converted the datasets to MS COCO-compliant format. We also saved the individual JSON annotation files for future reference. For example, they may be useful when annotation changes are needed, or when a different splitting of the dataset into training and validation subsets is required.

C. Environment setup

1) *Hardware*: Object detector training requires a lot of system resources, especially with the larger backbones and with increasing dataset sizes. We trained our models on supercomputer cluster that is part of a National Super Computing Grid. The supercomputer we used in our experiments employs 682 CPU nodes, and its performance can theoretically peak at 1.8 petaflops. Each node has two 20 core Intel Xeon Cascade Lake processors running at 2.1 GHz. It also features an “AI partition” that includes 80 GPU nodes with four Nvidia Tesla V100 32GB GPGPUs each, totaling 320 GPGPUs. The total theoretical performance of the GPGPUS is 2.7 petaflops. The nodes carry 384 GB of main memory and 3.6 TB quick local storage. For our experiments, we used one node that employs four Nvidia Tesla V100 32GB GPGPUs. We also performed some intermediate tests on our group’s HPC GPU mini-cluster. It features two Intel Xeon E5-2640 v4 CPUs totaling 20 cores running at 2.40 GHz, and includes eight Nvidia Tesla P100 16 GB GPGPUs. For our experiments, we used four Nvidia Tesla P100 16GB GPGPUs.

2) *Software*: In Table I we present a detailed list of software used during our experiments. The majority of software in our experiments is based on (or is written in) Python, and the frameworks in our experiments were implemented in PyTorch. To work with HPC clusters, we also needed to set up a Python environment with several needed libraries and packages. In order to achieve the setup, a virtual environment is required. Therefore, we used Conda [82] which is an open-source virtual environment and package manager. Furthermore, Conda enabled us to install and use different matching versions of packages and libraries, and it also isolated them to the specific virtual environment, making the experimentation and failure less painful and more streamlined. In particular, we used Miniconda3 variant since we did not require the features of the bulkier Anaconda3 package.

D. Model training

In order to train our CCTV camera detection models, we used the three frameworks that are state-of-the-art with top results. At the time of the experiments these are CenterMask2 [28], ATSS [34], and TridentNet [32]. Below we detail the experimental setups and parameters, that allowed us to evaluate and compare in the end six different object detectors, that are summarized in Table II. The best parameters values

TABLE I
DETAILS OF SOFTWARE AND TOOLS USED TO PERFORM THE EXPERIMENTS.

Software Name	Version	Purpose
Python	3.8.1	Python core
cuda toolkit	10.1.243	GPU programming
albumentations	0.4.3	Image augmentation library
numpy	1.18.1	Scientific computing package
OpenCV	4.2.0.32	Computer vision library
PyTorch	1.4.0	Machine learning framework
torchvision	0.5.0	Computer vision package
matplotlib	3.1.3	Graph visualizations
pycocotools	2.0	Tools for MS COCO
tqdm	4.42.1	Progress bar for terminal use
pillow	7.0.0	Imaging library (PIL fork)
cython	0.29.15	C-Extensions for Python
ninja	1.9.0	Small build system
pandas	1.0.1	Data analysis library
requests	2.23.0	HTTP library
scipy	1.4.1	Mathematics and science library
yacs	0.1.6	Configurations management system
Tensorboard	2.1.1	Training data capture
Detectron2	0.1.1	Object detection framework
QCC	8.3.0	GNU Compiler Collection
CUDA	10.1.168	Nvidia CUDA
labelme	4.2.9	Annotation tool
ATSS		ATSS - detector
CenterMask2		CenterMask - detector (PyTorch)
TridentNet		TridentNet - detector
detectron2-pipeline		Modular image processing pipeline

we chose were found by referencing the documentation, following best practices from the state-of-the-art, and performing multiple trial experiments.

1) *CenterMask2*: We trained our CenterMask2 [28], [29] with VoVNet-V2 [31] as backbone using the *V-57-eSE*, *V-99-eSE*, *V-39-eSe (lightweight)* variants. Throughout the paper we refer to these models as *CM2 Lite V-39*, *CM2 V-57*, and *CM2 V-99* respectively. First, we set the maximum iterations to 45000 with (i.e., 0.5x of the CenterMask2’s “1x learning rate” schedule which translates to default 90000 iterations). However, we found that we get even better results at 20000–30000 iterations checkpoint. In order to increase the training speed while still remaining under the Video-RAM (VRAM) threshold and also positively effect the results [83], we incremented the *batch size* from its default (16) to 24. The *base learning rate* was kept at default of 0.01., and enabled the multi-scale training at 640, 672, 704, 736, 768, and 800 pixels (measuring the smaller side of the input image). While keeping most of the configuration similar, the *V-39-eSe (lightweight)* has some specifics, such as accepting 580 and 600 pixel size input.

2) *ATSS*: When training our ATSS [34], we used the ResNet-50 [84] and ResNeXt-101 [85] backbones with multi-scale training and deformable convolutions. Both backbones used deformable convolutional networks version 2. Throughout the paper we refer to these models as *ATSS R-50*, and *ATSS X-101* respectively. The latter backbone has the *ResNeXt cardinality* set at 64, and the *bottleneck width* at 4d. Cardinality and bottleneck width are hyperparameters for aggregated residual transformations. They represent improvements made

for ResNeXt by Xie et al. [85] over the original ResNet [84] backbone. The cardinality is the number of paths inside the ResNeXt block. Bottleneck width is the number of individual channels in the bottleneck layers. The concept behind the ResNeXt block is *split-transform-aggregate*. The idea is that instead of growing the network deeper or wider, increasing the cardinality will increase accuracy and keep complexity of the network low [85]. Similarly to other models, we set the maximum iterations to 45000, with best results produced likewise around 20000–30000 iterations checkpoint. We left the *base learning rate* at 0.01, and used a *batch size* of 32. Since these are bigger backbones, we chose for multi-scale input image sizes of 640 and 800 pixels.

3) *TridentNet*: We performed training of our TridentNet [32] using the ResNet-101 [84] C4 backbone. Throughout the paper we refer to this model as *Trident R-101*. The C4 variant uses the features extracted from the ResNet’s fourth stage, while the fifth stage serves as *Region of Interest (RoI) heads* [81]. Similarly to other models, we set the maximum iterations to 45000, with best results produced likewise around 20000–30000 iterations checkpoint. We employed the standard *three-branch scheme* for the TridentNet multi-branch variant. Multi-scale training was also enabled at 640, 672, 704, 736, 768, and 800 pixels (measuring the smaller side of the input image). We also left the *base learning rate* at 0.02, and used a *batch size* of 24.

E. Various enhancements

1) *Image alterations*: We also propose and explore the effect of “image alteration” on the performance of our trained models [86]. By “image alterations” in our case we mean auto-adjust of contrast, equalizer, exposure, and hue-saturation. Results improvement with “image alteration” vary across the models. On the one hand, ATTS model seems to improve performance on contrast-enhanced images. Likewise, CenterMask2 detector enjoys a various degree of improvement in all cases of “image alteration”, however once again the contrast-enhanced images demonstrated top improvement results. On the other hand, TridentNet showed a decrease in confidence levels when used with “image alteration”, even though in isolated cases it enabled the model to correctly improve certain false negatives into true positives.

IV. ANALYSIS OF RESULTS

All the models were tested separately with both the validation dataset as well as with a separate testing dataset (see Section III-A). As mentioned earlier, the testing dataset mainly features images from street-level maps, since this corresponds to the intended use for the detector model. However, as we demonstrate in Appendix A, our system performs as expected even with arbitrary images acquired by third-parties using smartphones.

Table II shows the full detector and backbone combination along with the training iteration count for each model that provided the best performance for the whole training session.

TABLE II
DETECTOR CONFIGURATION, ITERATIONS COUNT, TRAINING AND INFERENCE TIMES (**BOLD**=BEST, UNDERLINE=WORST).

Detector	Best-result iterations (number)	Weights file size (MB)	Avg. train time / iter. (seconds)	Avg. inference time / image (seconds)
CM2 Lite V-39	20000	281.1	0.28	0.061
CM2 V-57	20000	551.4	0.81	0.089
CM2 V-99	30000	<u>776.0</u>	1.22	0.109
ATSS R-50	30000	264.1	0.48	0.064
ATSS X-101	22500	718.7	<u>2.40</u>	0.132
Trident R-101	20000	421.9	1.59	<u>0.169</u>

Additionally, Table II presents the timings for training and inference under each detection model.

A. Metrics for evaluation

To evaluate our models, we used *pycocotools* and MS COCO evaluator built into Detectron2 [25]. For all the models trained, we used the same evaluator. The metrics we use and present are the standard MS COCO’s [36] evaluation metrics. To evaluate the performance of a detector for the *detection performance*, MS COCO employs 12 characterizing metrics. *Average Precision (AP)* with MS COCO represents, in essence, a *mean Average Precision (mAP)* which takes the precision average across all the classes, all the while *localization accuracy* is built into the precision metrics. MS COCO’s standard measurement nowadays is largely represented by *Average Precision (AP)* and *Average Recall (AR)*, where the average is taken on 10 IoU thresholds from 0.5 to 0.95 with a 0.05 interval. AP across scales takes into account the area of pixels within the segmentation mask or the bounding box. In this context, based on the pixel size of the detected segmentation mask or the bounding box – “small objects” means areas up to 32×32 pixels, “medium objects” fit areas between 32×32 and 96×96 pixels, and “large objects” are represented by areas beyond 96×96 pixels. While AR also has the three metrics, the differentiating factor is the amount of detections per image – 1, 10, and 100. AR across scales is comparable to AP across scales [37]. The latest MS COCO metrics heavily weight on the localization with the Intersection over Union (IoU) threshold from 0.5 to 0.95. With our main and immediate use cases, the exact localization might not be absolutely necessary, therefore the precision with 0.5 IoU (i.e., AP@0.5) is the metric that is relevant in our case. However, in the spirit of evaluations and metrics used within the state-of-the-art detectors and backbones, we also collect, compute and present the most commonly used metrics (see Tables III IV).

In Table III we present the metrics (bounding box detection) for the “testing dataset”. The results suggest that the classification and the false positives are extremely good. For example, the AP@0.5 metric for all modes has excellent scores from high 80s percentile to mid 90s. At the same time, the results demonstrate that the localization accuracy (which is built into all precision metrics) suffers a bit. Therefore it affects some results and we can see that the precision metric with IoU from

0.5 to 0.95 takes a hit (i.e., $AP@0.5:0.95$), as for example is the case of ATSS X-101 model where its $AP@0.5:0.95$ tops at only 65,4%. The metrics showcase that smaller objects (e.g., images with CCTV cameras that are either distant or are really small size in real-life) seem to pose a challenge for all the models when compared to the medium size objects. The increase of object instances in an image does not seem to affect the models too much.

In Table IV we show the detection metrics (bounding box detection) for the “validation dataset”. Except for the case of small objects, the metrics for the “validation dataset” are not far superior when compared to the results of “testing dataset” (see Table III).

B. Visual result samples

To facilitate the understanding of successes, failures, and challenges faced by our detectors, we present in this section a selection of relevant samples along with some comments.

Figure 3 presents a relatively easy example of a side facing directed class instance. The minor challenge is the low contrast between the color of the camera and the background (i.e., color of the building). All detectors work well, while TridentNet achieves 100% confidence.



Fig. 3. Visual results (Ground Truth - 1 TP) (left to right): CenterMask2 V-57 - 1 TP (79%); ATSS X-101 - 1 TP (81%); TridentNet R-101 - 1 TP (100%)

Figure 4 features a side installation of a round class instance. Every model detects the camera correctly, and once again TridentNet achieves 100% confidence.



Fig. 4. Visual results (Ground Truth - 1 TP) (left to right): CenterMask2 V-57 - 1 TP (84%); ATSS X-101 - 1 TP (81%); TridentNet R-101 - 1 TP (100%)

Figure 5 shows a side facing directed class instance, which blends by color and texture with the background. None of the models detects the camera, and the outcome is a false

negative for each model. This indicates that the dataset requires instances for training that are considered “hard examples” such as this one.



Fig. 5. Visual results (Ground Truth - 1 TP) (left to right): CenterMask2 V-57 - 1 FN; ATSS X-101 - 1 FN; TridentNet R-101 - 1 FN. NOTE: Undetected TPs are marked with pink circle.

Figure 6 presents one of the worst-performing samples of the whole dataset. None of the models is able to detect side facing round class instance that also perfectly blends with the white background. At the same time, all of the detectors produce multiple false positives representing in fact light fixtures. One solution to this problem is to introduce into the training dataset the light fixtures (and similar potential false positive) as background (i.e., non-camera class labels). To further complicate this challenge, there is a growing number of hybrid installations where the CCTV cameras are combined with (Figure 7) or incorporated into light poles [87]. We leave the resolution for this challenge as future work.



Fig. 6. Visual results (Ground Truth - 1 TP) (left to right): CenterMask2 V-57 - 6 FP, 1 FN; ATSS X-101 - 3 FP, 1 FN; TridentNet R-101 - 2 FP, 1 FN. NOTE: Undetected TPs are marked with pink circle.

Next, we present some examples and results where we applied the “image alteration” techniques (Section III-E), thus seeking improvements in confidence levels and TP/TN/FP values that are as close as possible to the Ground Truth (GT).

For Figure 8, the CenterMask2 applied over the initial input image (omitted due to space constraints) detected all 3 TPs with the following confidence levels – 89%, 69%, 48%. With “image alteration” we can observe much better results with contrast, equalizer, and exposure modifications, where the equalizer case seems to bring the optimal result.

At the same time, “image alteration” does not always bring result improvements. For example, as seen with Figure 9 TridentNet mode had no improvements on the detection, and the other models produced similarly unimproved outputs.

TABLE III
RESULTS FOR BOUNDING BOX DETECTION WITH THE *TEST DATASET* (**BOLD**=BEST, UNDERLINE=WORST).

Detector	AP@0.5	AP@0.5:0.95	APs	APm	AR 1	AR 10	ARs	ARm
CM2 Lite V-39	88,2%	63,8%	65,4%	68,7%	61,0%	73,4%	69,7%	78,8%
CM2 V-57	89,7%	62,9%	62,8%	66,3%	61,5%	71,5%	65,7%	79,5%
CM2 V-99	90,1%	64,9%	64,3%	70,2%	61,5%	72,9%	68,1%	79,7%
ATSS R-50	86,5%	58,2%	57,4%	63,9%	56,8%	66,0%	60,7%	73,5%
ATSS X-101	91,1%	65,4%	64,4%	70,1%	61,6%	72,3%	67,2%	79,4%
Trident R-101	88,3%	58,7%	<u>56,0%</u>	65,4%	<u>56,3%</u>	<u>65,8%</u>	<u>58,5%</u>	76,0%

TABLE IV
RESULTS FOR BOUNDING BOX DETECTION WITH THE *VALIDATION DATASET* (**BOLD**=BEST, UNDERLINE=WORST).

Detector	AP@0.5	AP@0.5:0.95	APs	APm	API	AR 1	AR 10	ARs	ARm	ARI
CM2 Lite V-39	93,9%	69,9%	49,9%	72,1%	77,1%	71,1%	76,5%	54,5%	77,5%	85,6%
CM2 V-57	95,6%	74,5%	57,4%	75,9%	81,1%	74,6%	80,3%	60,5%	81,0%	88,0%
CM2 V-99	95,0%	73,3%	55,5%	74,0%	82,1%	74,0%	79,5%	58,8%	79,4%	89,3%
ATSS R-50	93,2%	71,7%	52,3%	74,4%	77,6%	72,9%	78,2%	55,4%	80,0%	86,3%
ATSS X-101	94,3%	73,1%	54,6%	76,0%	78,0%	74,2%	79,6%	57,8%	81,2%	86,8%
Trident R-101	94,0%	70,3%	52,7%	<u>70,9%</u>	79,8%	73,0%	77,6%	55,6%	78,7%	86,8%



Fig. 7. Example of a hybrid installation consisting of a light pole combined with a CCTV camera. Our TridentNet model works well with a detection confidence of 97% of the “round class” instance, and avoids the potential “directed class” false positive represented by the light fixture below the camera.

V. DISCUSSION

In this section we discuss some practical applications of our present work, as well as some ethical aspects and potential challenges.

A. Practical applications

1) *Fast and accurate CCTV camera annotations*: Crowd-sourcing is a proven and effective method for fast, accurate, and cost-effective for image labeling and annotation, and generic computer vision and machine learning tasks [88]–[92]. Google is using a similar approach integrated into its reCAPTCHA V2 [93], [94]. As presented in Figure 10, we

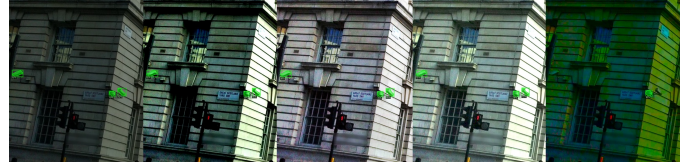


Fig. 8. Image alterations with CenterMask (Ground Truth - 3 TP) (left to right): Original - 3 TP (92%, 83%, 52%); Contrast - 3 TP (92%, 54%, 91%); Equalizer - 3 TP (84%, 81%, 90%); Exposure - 3 TP (92%, 86%, 73%); Saturation - 1 TP (85%), 2 FN



Fig. 9. Image alterations with TridentNet (Ground Truth - 1 TP) (left to right): Original - 1 FN; Contrast - 1 FN; Equalizer - 1 FN; Exposure - 1 FN; Saturation - 1 FN. NOTE: Undetected TPs are marked with pink circle.

propose an improvement to the current reCAPTCHA V2 system. Our proposed improvement could ask the users of reCAPTCHA to “*Select all images with **CCTV cameras***”, hence leveraging reCAPTCHA’s unified infrastructure and algorithms to better and faster help to annotate and validate the CCTV camera objects in Google Street View imagery as well as other image datasets. To our knowledge, at the time of this writing there is no such publicly available feature in Google’s reCAPTCHA.

2) *Global and instant mapping of CCTV locations and areas*: On the one hand, at present there are multiple projects and data-sources that provide the geo-location mapping of CCTV cameras. Some of these projects are open-source and crowd-sourced [95], [96], while some others are open-data resources provided by city administrations and country govern-

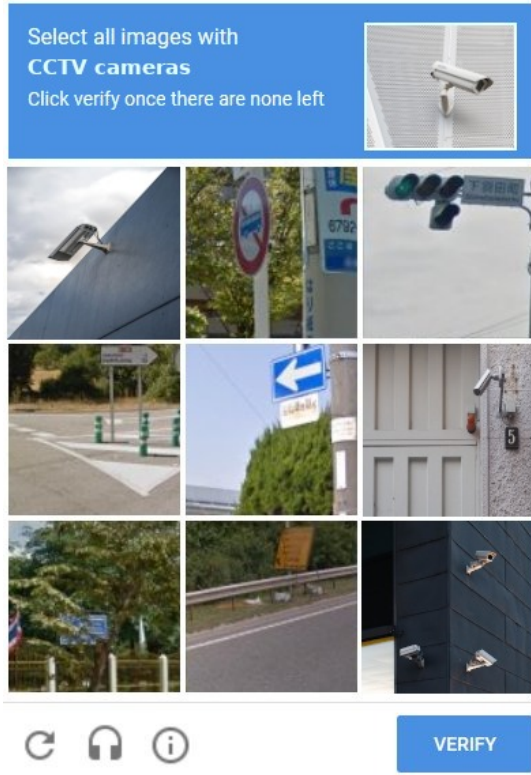


Fig. 10. Our proposed vision for a novel reCAPTCHA V2 extension offering “Select all images with **CCTV cameras**” to better and faster help annotate and validate the CCTV camera objects in Google Street View imagery.

ments [97]–[100]. However, all of these feature a set of major limitations, as follows. First, all these approaches cover a very limited geographical area (e.g., maximum a city). Second, the data-sources and projects are globally uncoordinated. Therefore the data formats along with the exposed characteristics of the respective maps and CCTV cameras vary dramatically across the board. Third, crowd-sourced project rely heavily on human contributions of data, while governmental data-sources rely on human administration of data. Such an approach is highly unscalable for maintenance and development of the datasets, and exposes the data to human error and (un)intentional manipulations. Fourth, those datasets are rarely kept up-to-date and they inherently cannot reflect the instant changes in the addition, removal, reposition of CCTV cameras (e.g., due to infrastructure changes, construction).

On the other hand, our CCTV camera object detector can be applied to a global source of street-level imagery such as Google Street View, OpenStreetCam, Mapillary. This allows fast mapping and localization of most street-level (and even indoor ³) CCTV cameras, therefore instantly creating and maintaining a global up-to-date (and historical [102]) map of CCTV cameras. At the same time, our CCTV camera object detector can be used to validate the accuracy and truthfulness of the crowd-sourced and open-data datasets. To achieve this,

³Our approach can also detect and map indoor CCTV cameras thanks to panoramas in Google Street View supplied by Google and its users [101].

an automated process picks each CCTV camera entry from a dataset, retrieves the relevant and closest street-level and geo-tagged imagery, applies our CCTV camera object detector, and finally validates if the dataset is correct and contains up-to-date information.

3) *CCTV-aware privacy-/safety-focused route planning and navigation*: Once the CCTV cameras can be accurately detected, and instantly located and mapped based on street-level imagery ⁴ (see Section V-A2), the system is ready for one of the most important and relevant application – *CCTV-aware route planning and navigation*.

At present, there is a myriad of route planning algorithms, software, and services ⁵ [103]–[108]. However, to the best of our knowledge, none of the currently available algorithms, software, and services provide *CCTV-aware* route planning and navigation. To the best of our knowledge, we are the first to propose and work on such features at present, and we are unaware of any project or service developing or offering such route planning options.

In Figures 12, 13 we demonstrate some real-world use-cases of such a CCTV-aware route planner. The samples contain the mapping and labeling of location, type (e.g., *round camera*, *directed camera*), and field of view. This mapping and labeling is achieved using the previously detailed CCTV camera object detectors (Sections III, IV). The user first have the option to select the type of *CCTV-aware routing*, as presented in Figure 11.

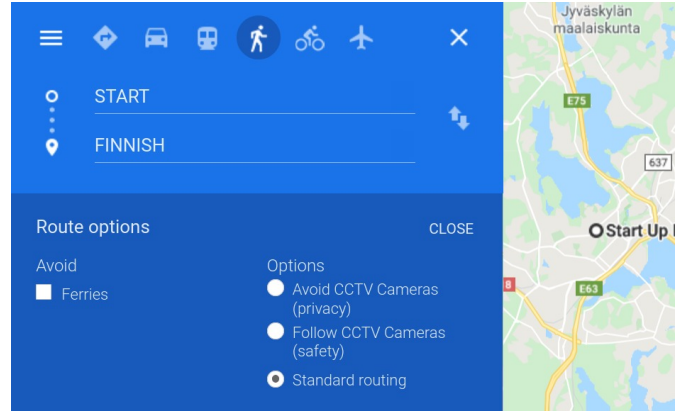


Fig. 11. Our proposed vision for a novel map navigation that provides the users both privacy (“Avoid CCTV Cameras (privacy-first)”) and safety (“Follow CCTV Cameras (safety-first)”) route planning options.

Then, if the user selects the “*Follow CCTV Cameras (safety-first)*” option the system would provide a route as in Figure 12. As already mentioned, current route planning solutions provide *CCTV-unaware* algorithms, therefore the systems we tested (e.g., Google Maps) provided most of the times the same non-privacy-friendly route as in Figure 12. At the same time, with our *CCTV-aware* route planning proposal, the user may alternatively select “*Avoid CCTV Cameras (privacy-first)*”.

⁴Also can be applied to geo-tagged photos and videos.

⁵Provided as a wide variety of open-source, closed-source, online, offline, free, and commercial solutions.

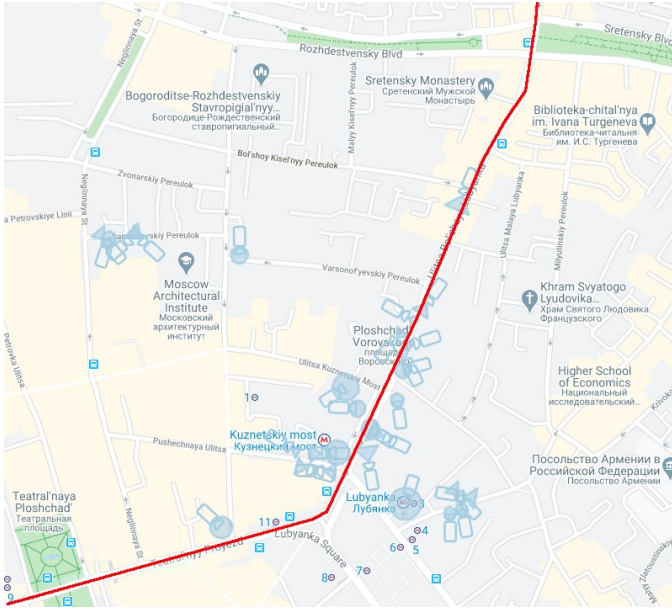


Fig. 12. CCTV-aware routing system providing route for “*Follow CCTV Cameras (safety-first)*” user option, routing the user through the hot-spot view of tens of CCTV cameras. NOTE: We used street-level imagery at the given geo-location and mapped the real-life positioning of CCTV cameras in the given area.

Therefore, the system would provide a better route for that scenario as depicted in Figure 13.

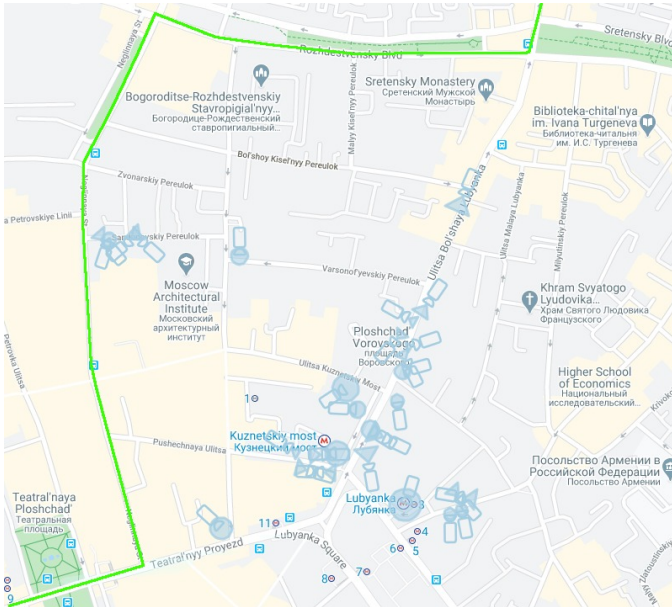


Fig. 13. CCTV-aware routing system providing route for “*Avoid CCTV Cameras (privacy-first)*” user option, routing the user away from the “prying eyes” of tens of CCTV cameras (depicted in light-blue). NOTE: We used street-level imagery at the given geo-location and mapped the real-life positioning of CCTV cameras in the given area.

4) *Real-time CCTV detection on mobile/IoT devices:* Finally, one more application of the presented object detector is its use for real-time CCTV camera detection on smartphones,

mobile equipment (e.g., robots, drones), and other IoT/edge devices (e.g., RaspberryPi, Arduino, ESP32). For this purpose, our object detectors could be configured and trained for low-power devices using, for example, TinyML hardware with TensorFlow Lite [109], [110], and we leave this as part of our future work. One use-case could be the drones equipped with tiny/lite versions of our detection models could fly around the corner or down the street to first detect and map the CCTV areas. Another use-case could be users equipped with smartphones or IoT/edge devices that continuously runs the tiny/lite object detector over the device’s camera video feed. The device would then alert the user (e.g., via sound, vibration, light) when it detects in real-time a CCTV camera in its field of view, therefore providing the user a chance to change course and make a more informed decision.

In this context, we also tested our system (namely the ATSS X-101 and Trident R-101 models) against the real-world journalist experiment by Pasley [2], where the “ground truth” consists of 39 TPs (i.e., CCTV cameras). Running ATSS X-101 detector resulted in 33 TPs + 0 FPs + 6 FNs. Applying Trident R-101 model produced 33 TPs + 1 FPs + 6 FNs. Both models presented an F1-score of 91.7%, and while their TPs and FNs counts are the same, the actual distribution of TPs and FNs across the input images slightly differs. Therefore, we also evaluated our system using a “sensor fusion” approach, where the best results from both the detectors (i.e., “sensors”) are combined (i.e., “fused”) together for an enhanced final result. In this case, our system achieves 35 TPs + 0 FPs + 4 FNs with an F1-score of 94.6%. A visual results subset from our experiment can be seen in Appendix A. This therefore underpins once again that our technology could be useful as *privacy-first* early warning system against CCTV cameras for real-life use by third-parties and users.

B. Technical challenges

Based on our real-world and street imagery observations, light equipment (e.g., light poles, light fixtures) many time look very similar to CCTV cameras. This makes it challenging to certainly distinguish between CCTV cameras and light equipment even to an experienced human observer. Figure 6, which is the worst-performing and where most of the False Positives are in fact light fixtures, is a perfect example that such a scenario poses challenges to computer vision as well. At the same time, there seems to be a growing trend to have streetlights with embedded CCTV cameras [87]. We think this may pose additional challenges (not insurmountable though) for most-accurate detection of CCTV cameras in real-life scenarios.

C. Ethical aspects and potential abuse

On the one hand, there are less technological domains where a system inspired by our work could be applied. For example, the case of Novichok (A-234) poisoning in Salisbury (UK) of the former Russian military intelligence officer Sergei Skripal, and his daughter Yulia Skripal, by what is believed

to be two officers of Russian GRU ⁶ – “Ruslan Boshirov” (supposed real name Anatoliy Chepiga [111]) and “Alexander Petrov” (supposed real name Alexander Mishkin [112]) – is surreal and beyond infamous [113]. Following the attack and the international diplomatic fallout featuring sanctions and diplomatic expulsions, the Law Enforcement agencies and investigative think-tank organizations (e.g., Bellingcat) reconstructed the complete routes with exact geo-positions, timestamps, and visual proof of main suspects *with the heavy use of state- and privately-owned CCTV cameras* [114]. In this context, some readers may object that future potential delinquents could use a system similar to ours in order to map the CCTV cameras within a planned operation area (if not already available), and then use it to carefully generate a specific route that provides close to 100% anonymity. We argue our point of view on this at the end of this section.

On the other hand, there are offensive cybersecurity scenarios (possible but unlikely in the immediate future), where our technology could be potentially used. The scenario works under the following attack assumptions:

- it is completely autonomous (i.e., *no human operators*)
- it involves offensive drones equipped with CCTV camera object detector (*attackers*) (see Section V-A4)
- it targets highly-valuable air-gapped network(s) to exfiltrate data from (*victims*)

Attack description: The drones use the object detector to identify CCTV cameras and approach them. Once approached, the drones would send a “backdoor knock” signal (e.g., visual, sound, infra-red) to the camera [5], [115]. If a particular CCTV camera was internally compromised and connected to an isolated network segment that contains a latent malware implant (e.g., APT), the malware activates when camera receives the “backdoor knock” signal. The malware could also be implanted in the CCTV camera itself via IoT malware and firmware modifications [6], [116], [117]. To complete the attack, the drones with such CCTV camera object detection and data-exfiltration capabilities follow the *air-jumper* attack described by Guri and Bykhovsky [115].

All in all, we argue that while our CCTV camera object detector is designed to be used for *positive impact*, the potential of our proposed system being misused is similar and comparable to any other system (e.g., Kali Linux, Metasploit), method (e.g., penetration testing, reverse engineering), or device (e.g., kitchen knives in supermarkets). Additionally, we argue that the benefits of our system for the majority of *positive impact* applications outweigh the risks of misuse for a fraction of *negative impact* applications (where we believe the perpetrators to be able to find other ingenious ways for illegal or unethical activity, should a system like ours not exist).

VI. CONCLUSION

In this paper we presented the first state-of-the-art computer vision object detectors aiming to accurately identify CCTV

cameras in images and video frames. Our object detectors currently achieve an accuracy between 91,1% – 95,6%. To build our system, we used and evaluated in parallel several state-of-the-art computer vision frameworks and backbones. To train our system, we manually collected, triaged and annotated 3401 CCTV camera images, for a total of 2244 directed class instances and 1742 round class instances.

Furthermore, we presented the first known prototypes of *CCTV-aware route planning and navigation*. These prototypes are motivated and powered by the core object detectors presented above, and can be used at the same time for both *privacy-first* (avoid CCTV cameras) as well as *safety-first* (follow CCTV cameras) route planning.

Finally, with this work, we hope to motivate in several ways the communities of researchers, practitioners, policy-makers, and end-users. First and more general is to focus the debates and policy-making related to privacy and safety of CCTV cameras towards a more science-, technology- and research-driven ground. Second is to encourage the improvement of our object detectors and techniques presented, so that they can be immediately incorporated at a larger scale, both in cloud and edge applications, and for the greater privacy benefit. With these in mind, we release the relevant artefacts (e.g., code, datasets, trained models, and documentation) at: <https://github.com/Fuziih> and <https://etsin.fairdata.fi/dataset/d2d2d6e2-0b5c-46e0-8833-53d8a24838a0> (*urn:nbn:fi:att:258ce5ad-9501-46b9-a707-c1f59689ee10*).

ACKNOWLEDGMENTS

We acknowledge grants of computer capacity from the Finnish Grid and Cloud Infrastructure (FGCI) (persistent identifier *urn:nbn:fi:research-infras-2016072533*).

⁶ Glavnoe Razvedyvatelnoe Upravlenie – Main Directorate of the General Staff of the Armed Forces of the Russian Federation, formerly the Main Intelligence Directorate.

REFERENCES

- [1] H. Turtiainen, "State-of-the-art object detection model for detecting CCTV and video surveillance cameras from images and videos," Master's thesis, University of Jyväskylä, Jyväskylä, Finland, 2020. [Online]. Available: <http://urn.fi/URN:NBN:fi:juu-202005253430>
- [2] J. Pasley, "I documented every surveillance camera on my way to work in New York City, and it revealed a dystopian reality," <https://www.businessinsider.com/how-many-security-cameras-in-new-york-city-2019-12>, Dec 2019.
- [3] E. Cosgrove, "One billion surveillance cameras will be watching around the world in 2021," <https://cnbc.com/2019/12/06/one-billion-surveillance-cameras-will-be-watching-globally-in-2021.html>.
- [4] A. Glinsky, *Theremin: ether music and espionage*. University of Illinois Press, 2000.
- [5] A. Costin, "Security of CCTV and video surveillance systems: Threats, vulnerabilities, attacks, and mitigations," in *6th International Workshop on Trustworthy Embedded Devices (TrustED)*, 2016.
- [6] M. Antonakakis et al., "Understanding the mirai botnet," in *26th USENIX Security Symposium (USENIX Security 17)*. USENIX Association, 2017.
- [7] Electronic Frontier Foundation, "Street-Level Surveillance – Surveillance Cameras," <https://www EFF.org/pages/surveillance-cameras>.
- [8] C. Slobogin, "Public privacy: camera surveillance of public places and the right to anonymity," *Miss. LJ*, vol. 72, p. 213, 2002.
- [9] B. v. S.-T. Larsen, *Setting the watch: privacy and the ethics of CCTV surveillance*. Bloomsbury Publishing, 2011.
- [10] J. Ryberg, "Privacy rights, crime prevention, cctv, and the life of mrs aremac," *Res Publica*, vol. 13, no. 2, pp. 127–143, 2007.
- [11] B. J. Gool, "Privacy rights and public spaces: Cctv and the problem of the unobservable observer," *Criminal Justice Ethics*, vol. 21, no. 1, pp. 21–27, 2002.
- [12] G. Gerrard and R. Thompson, "Two million cameras in the uk," *CCTV image*, vol. 42, no. 10, p. e2, 2011.
- [13] M. McCahill and C. Norris, "Cctv in london," *Report deliverable of UrbanEye project*, 2002.
- [14] D. Barrett, "One surveillance camera for every 11 people in Britain, says CCTV survey."
- [15] "How Many CCTV Cameras in London?" <https://www.caughtoncamera.net/news/how-many-cctv-cameras-in-london/>.
- [16] B. Karas, "Americans Vastly Underestimate Being Recorded on CCTV," <https://ipvm.com/reports/america-cctv-recording>.
- [17] P. Bischoff, "Surveillance camera statistics: which cities have the most CCTV cameras?" <https://www.comparitech.com/vpn-privacy/the-worlds-most-surveilled-cities/>.
- [18] E. Heathcote, "Artists and activists offer privacy hope as facial recognition spreads," <https://www.ft.com/content/15fb3c5a-2178-11ea-b8a1-584213ee7b2b>, 2020.
- [19] M. Lothian-McLean, "These activists use makeup to defy mass surveillance," https://i-d.vice.com/en_uk/article/jge5jg/dazzle-club-surveillance-activists-makeup-marches-london-interview.
- [20] M. Pollard, "Even mask-wearers can be ID'd, China facial recognition firm says," <https://reuters.com/article/us-health-coronavirus-facial-recognition/even-mask-wearers-can-be-idd-china-facial-recognition-firm-says-idUSKBN20W1>.
- [21] D. Onoro-Rubio and R. J. López-Sastre, "Towards perspective-free object counting with deep learning," in *European Conference on Computer Vision*. Springer, 2016.
- [22] J. Fuentes-Pacheco, J. Ruiz-Ascencio, and J. M. Rendón-Mancha, "Visual simultaneous localization and mapping: a survey," *Artificial intelligence review*, vol. 43, no. 1, pp. 55–81, 2015.
- [23] G. Verhoeven, M. Doneus, C. Briese, and F. Vermeulen, "Mapping by matching: a computer vision-based approach to fast and accurate georeferencing of archaeological aerial photographs," *Journal of Archaeological Science*, vol. 39, no. 7, pp. 2060–2070, 2012.
- [24] A. Frome, G. Cheung, A. Abdulkader, M. Zennaro, B. Wu, A. Bissacco, H. Adam, H. Neven, and L. Vincent, "Large-scale privacy protection in Google Street View," in *12th international conference on computer vision*. IEEE, 2009.
- [25] Y. Wu, A. Kirillov, F. Massa, W.-Y. Lo, and R. Girshick, "Detectron2: A PyTorch-based modular object detection library," <https://ai.facebook.com/blog/detectron2-a-pytorch-based-modular-object-detection-library/>.
- [26] R. Girshick, I. Radosavovic, G. Gkioxari, P. Dollár, and K. He, "Detectron," 2018.
- [27] F. Massa and R. Girshick, "Faster R-CNN and Mask R-CNN in PyTorch 1.0," Facebook Research, Apr. 2020.
- [28] Y. Lee and J. Park, "CenterMask2: Real-Time Anchor-Free Instance Segmentation," Apr. 2020.
- [29] —, "Centermask: Real-time anchor-free instance segmentation."
- [30] Z. Tian, C. Shen, H. Chen, and T. He, "FCOS: Fully Convolutional One-Stage Object Detection," 2019.
- [31] Y. Lee, J. won Hwang, S. Lee, Y. Bae, and J. Park, "An Energy and GPU-Computation Efficient Backbone Network for Real-Time Object Detection," 2019.
- [32] Y. Li, Y. Chen, N. Wang, and Z. Zhang, "Scale-aware trident networks for object detection," 2019.
- [33] F. Yu and V. Koltun, "Multi-scale context aggregation by dilated convolutions," 2015.
- [34] S. Zhang, C. Chi, Y. Yao, Z. Lei, and S. Z. Li, "Bridging the gap between anchor-based and anchor-free detection via adaptive training sample selection," 2019.
- [35] T.-Y. Lin, P. Goyal, R. Girshick, K. He, and P. Dollár, "Focal loss for dense object detection," 2017.
- [36] T.-Y. Lin, M. Maire, S. Belongie, J. Hays, P. Perona, D. Ramanan, P. Dollár, and C. L. Zitnick, "Microsoft COCO: Common objects in context," in *European Conference on Computer Vision*. Springer, 2014.
- [37] "COCO - Common Objects in Context," <http://cocodataset.org/#home>.
- [38] M. Everingham, L. V. Gool, C. K. I. Williams, J. Winn, and A. Zisserman, "The PASCAL Visual Object Classes (VOC) challenge," 2010.
- [39] "The PASCAL Visual Object Classes," <http://host.robots.ox.ac.uk/pascal/VOC/>.
- [40] M. Everingham and J. Winn, "The PASCAL Visual Object Classes Challenge 2012 (VOC2012) Development Kit," 2012.
- [41] L. Jiao, F. Zhang, F. Liu, S. Yang, L. Li, Z. Feng, and R. Qu, "A survey of deep learning-based object detection," *IEEE Access*, vol. 7, 2019. [Online]. Available: <http://dx.doi.org/10.1109/ACCESS.2019.2939201>
- [42] O. Russakovsky, J. Deng, H. Su, J. Krause, S. Satheesh, S. Ma, Z. Huang, A. Karpathy, A. Khosla, M. Bernstein, A. C. Berg, and L. Fei-Fei, "Imagenet large scale visual recognition challenge," 2014.
- [43] A. Kuznetsova, H. Rom, N. Alldrin, J. Uijlings, I. Krasin, J. Pont-Tuset, S. Kamali, S. Popov, M. Mallocci, A. Kolesnikov, T. Duerig, and V. Ferrari, "The open images dataset v4: Unified image classification, object detection, and visual relationship detection at scale," *IJCV*, 2020.
- [44] "Open Images Dataset V6 + Extensions," <https://storage.googleapis.com/openimages/web/index.html>.
- [45] D. Anguelov, C. Dulong, D. Filip, C. Frueh, S. Lafon, R. Lyon, A. Ogale, L. Vincent, and J. Weaver, "Google street view: Capturing the world at street level," *Computer*, vol. 43, no. 6, pp. 32–38, 2010.
- [46] S. I. L. Paiva, "Inferring urban indicators through computer vision on google street view," 2018.
- [47] Z. Wojna, A. N. Gorban, D.-S. Lee, K. Murphy, Q. Yu, Y. Li, and J. Ibarz, "Attention-based extraction of structured information from street view imagery," in *14th IAPR International Conference on Document Analysis and Recognition (ICDAR)*. IEEE, 2017.
- [48] K. Hara, V. Le, and J. Froehlich, "A feasibility study of crowdsourcing and Google Street View to determine sidewalk accessibility," in *14th international ACM SIGACCESS conference on Computers and accessibility*, 2012.
- [49] —, "Combining crowdsourcing and Google Street View to identify street-level accessibility problems," in *SIGCHI conference on human factors in computing systems*, 2013.
- [50] K. Hara, J. Sun, R. Moore, D. Jacobs, and J. Froehlich, "Tohme: detecting curb ramps in Google Street View using crowdsourcing, computer vision, and machine learning," in *27th annual ACM symposium on User interface software and technology*, 2014.
- [51] K. Hara, S. Azenkot, M. Campbell, C. L. Bennett, V. Le, S. Pannella, R. Moore, K. Minckler, R. H. Ng, and J. E. Froehlich, "Improving public transit accessibility for blind riders by crowdsourcing bus stop landmark locations with Google Street View: An extended analysis," *ACM Transactions on Accessible Computing (TACCESS)*, 2015.
- [52] A. R. Zamir and M. Shah, "Accurate image localization based on Google Maps Street View," in *European Conference on Computer Vision*. Springer, 2010.
- [53] M. Turk and A. Pentland, "Face recognition using eigenfaces," in *Proceedings of IEEE computer society conference on computer vision and pattern recognition*, 1991.

- [54] V. Bruce and A. Young, "Understanding face recognition," *British journal of psychology*, vol. 77, no. 3, pp. 305–327, 1986.
- [55] R. Brunelli and T. Poggio, "Face recognition: Features versus templates," *IEEE transactions on pattern analysis and machine intelligence*, vol. 15, no. 10, pp. 1042–1052, 1993.
- [56] T. Ahonen, A. Hadid, and M. Pietikäinen, "Face recognition with local binary patterns," in *European conference on computer vision*, 2004.
- [57] A. K. Jain and S. Z. Li, *Handbook of face recognition*, 2011.
- [58] P. J. Phillips, P. J. Flynn, T. Scruggs, K. W. Bowyer, J. Chang, K. Hoffman, J. Marques, J. Min, and W. Worek, "Overview of the face recognition grand challenge," in *Computer society conference on computer vision and pattern recognition*. IEEE, 2005.
- [59] O. M. Parkhi, A. Vedaldi, and A. Zisserman, "Deep face recognition," 2015.
- [60] L. J. Halawa, A. Wibowo, and F. Ernawan, "Face Recognition Using Faster R-CNN with Inception-V2 Architecture for CCTV Camera," in *2019 3rd International Conference on Informatics and Computational Sciences (ICICoS)*, 2019.
- [61] S. Ren, K. He, R. Girshick, and J. Sun, "Faster r-cnn: Towards real-time object detection with region proposal networks," 2015.
- [62] S. Bah and F. Ming, "An improved face recognition algorithm and its application in attendance management system," *Array*, vol. 5, 2019.
- [63] M. Mileva and A. Burton, "Face search in cctv surveillance," *Cognitive research: principles and implications*, vol. 4, no. 3, 2019.
- [64] A. Kofman, "Losing Face How a Facial Recognition Mismatch Can Ruin Your Life," <https://theintercept.com/2016/10/13/how-a-facial-recognition-mismatch-can-ruin-your-life/>, 2016.
- [65] A. Kaganstih, "'Big Brother' for sale, or the 'Black Markets' of a 'Safe Smart City'." Video report. (Bol'shoj Brat optom i v roznicu, ili Chernyj rynek Bezopasnogo goroda. Videoreportazh.), <https://mbk.news/suzhet/bolshoj-brat-optom-i-v-roznicu/>, Dec 2019.
- [66] M. Bishop and C. Gates, "Defining the insider threat," in *4th annual workshop on Cyber security and information intelligence research*, 2008.
- [67] L. Spitzner, "Honeypots: Catching the insider threat," in *19th Annual Computer Security Applications Conference*. IEEE, 2003.
- [68] A. Cui and S. J. Stolfo, "A quantitative analysis of the insecurity of embedded network devices: results of a wide-area scan," in *26th Annual Computer Security Applications Conference*, 2010.
- [69] A. Costin, J. Zaddach, A. Francillon, and D. Balzarotti, "A large-scale analysis of the security of embedded firmwares," in *23rd USENIX Security Symposium*, 2014.
- [70] A. Costin, A. Zarras, and A. Francillon, "Automated dynamic firmware analysis at scale: a case study on embedded web interfaces," in *11th ACM on Asia Conference on Computer and Communications Security*, 2016.
- [71] C. Heffner, "Exploiting surveillance cameras," 2013.
- [72] A. Costin, "Poor Man's Panopticon: Mass CCTV surveillance for the masses," *PowerOfCommunity*, November, 2013.
- [73] S. Shekhan and A. Harutyunyan, "To Watch Or To Be Watched. Turning your surveillance camera against you," *HITB AMS*, 2013.
- [74] "Insecam – online cameras directory," <https://insecam.org>, 2013.
- [75] H. Xu, F. Xu, and B. Chen, "Internet protocol cameras with no password protection: An empirical investigation," in *International Conference on Passive and Active Network Measurement*, 2018.
- [76] B. Krebs, "Source code for IoT botnet 'Mirai' released," *KrebsOnSecurity*, (Oct. 2016). Retrieved Feb, 2016.
- [77] "OpenStreetCam," <https://openstreetcam.org/>.
- [78] "Google Street View," <https://www.google.com/streetview/explore/>.
- [79] K. Wada, "labelme: Image Polygonal Annotation with Python," <https://github.com/wkentaro/labelme>, 2016.
- [80] B. Russell, A. Torralba, K. Murphy, and W. Freeman, "Labelme: A database and web-based tool for image annotation," *International Journal of Computer Vision*, vol. 77, no. 1-3, pp. 157–173, 2008. [Online]. Available: <http://dx.doi.org/10.1007/s11263-007-0090-8>
- [81] K. He, G. Gkioxari, P. Dollár, and R. Girshick, "Mask R-CNN," 2017.
- [82] "Conda — conda 4.8.3 documentation," <https://docs.conda.io/projects/conda/en/latest/>.
- [83] P. M. Radiuk, "Impact of training set batch size on the performance of convolutional neural networks for diverse datasets," *Information Technology and Management Science*, vol. 20, no. 1, pp. 20–24, 2017.
- [84] K. He, X. Zhang, S. Ren, and J. Sun, "Deep Residual Learning for Image Recognition," 2015.
- [85] S. Xie, R. Girshick, P. Dollár, Z. Tu, and K. He, "Aggregated Residual Transformations for Deep Neural Networks," in *Conference on Computer Vision and Pattern Recognition*. Honolulu, HI: IEEE, 2017.
- [86] X. Chen, "Image enhancement effect on the performance of convolutional neural networks," 2019.
- [87] L. Winkley and T. Figueroa, "San Diego has more than 3,000 cameras on streetlights," <https://www.sandiegouniontribune.com/news/public-safety/story/2020-03-01/san-diego-has-3-000-cameras-on-street-lights-do-they-target-any>.
- [88] A. Kovashka, O. Russakovsky, L. Fei-Fei, and K. Grauman, "Crowdsourcing in computer vision," *arXiv preprint arXiv:1611.02145*, 2016.
- [89] C. Wah, "Crowdsourcing and its applications in computer vision," *University of California, San Diego*, 2006.
- [90] P. Welinder and P. Perona, "Online crowdsourcing: rating annotators and obtaining cost-effective labels," in *Computer Society Conference on Computer Vision and Pattern Recognition-Workshops*. IEEE, 2010.
- [91] R. Di Salvo, D. Giordano, and I. Kavasidis, "A crowdsourcing approach to support video annotation," in *International Workshop on Video and Image Ground Truth in Computer Vision Applications*, 2013.
- [92] J. Deng, J. Krause, and L. Fei-Fei, "Fine-grained crowdsourcing for fine-grained recognition," in *IEEE conference on computer vision and pattern recognition*, 2013.
- [93] L. Von Ahn, B. Maurer, C. McMillen, D. Abraham, and M. Blum, "recaptcha: Human-based character recognition via web security measures," *Science*, vol. 321, no. 5895, pp. 1465–1468, 2008.
- [94] "reCAPTCHA help," <https://support.google.com/recaptcha/?hl=en>.
- [95] Tramaci, "Anopticon – Mappa delle Telecamere – 'Big Brother' Viewer – Il grande fratello (secondo orwell) si sta espandendo." <http://tramaci.org/anopticon/>.
- [96] OpenStreetMap, "Camera Objects," <https://wiki.openstreetmap.org/w/index.php?search=camera&title=Special%3ASearch&go=Go>.
- [97] "Gorodskaja sistema videonabljudenija (Moskva) – City video-surveillance system (Moscow)," <https://video.dit.mos.ru/about/>.
- [98] "Carte de l'implantation des camras de vidéoverbalisation à Paris," <https://www.data.gouv.fr/fr/reuses/carte-de-limplantation-des-cameras-de-videoverbalisation-a-paris/>.
- [99] "Vidéoprotection - Implantation des caméras," <https://www.data.gouv.fr/fr/datasets/videoprotection-implantation-des-cameras-kml-ods/>.
- [100] "The spatial distribution of open-street CCTV in the Brussels-Capital Region," <https://journals.openedition.org/brussels/1427?lang=en>.
- [101] Google, "Publish and connect 360 photos with the Street View app," <https://support.google.com/maps/answer/7011737?hl=en>, 2018.
- [102] C. Smith, "Travel back in time with Google Street View," <http://home.bt.com/tech-gadgets/internet/travel-back-in-time-with-google-street-view-11363960715817>, 2018.
- [103] OpenStreetMap, "Routing/online routers," https://wiki.openstreetmap.org/wiki/Routing/online_routers.
- [104] —, "Routing/offline routers," https://wiki.openstreetmap.org/wiki/Routing/offline_routers.
- [105] D. Luxen and C. Vetter, "Real-time routing with OpenStreetMap data," in *Proceedings of the 19th ACM SIGSPATIAL international conference on advances in geographic information systems*, 2011.
- [106] D. Delling, P. Sanders, D. Schultes, and D. Wagner, "Engineering route planning algorithms," in *Algorithmics of large and complex networks*. Springer, 2009.
- [107] H. Bast, D. Delling, A. Goldberg, M. Müller-Hannemann, T. Pajor, P. Sanders, D. Wagner, and R. F. Werneck, "Route planning in transportation networks," in *Algorithm engineering*. Springer, 2016.
- [108] R. J. Szczerba, P. Galkowski, I. S. Glicktein, and N. Ternullo, "Robust algorithm for real-time route planning," *IEEE Transactions on Aerospace and Electronic Systems*, vol. 36, no. 3, pp. 869–878, 2000.
- [109] C. R. Banbury, V. J. Reddi, M. Lam, W. Fu, A. Fazel, J. Holleman, X. Huang, R. Hurtado, D. Kanter, A. Lokhtov et al., "Benchmarking TinyML Systems: Challenges and Direction," *arXiv preprint arXiv:2003.04821*, 2020.
- [110] X. Zhang, Y. Wang, and W. Shi, "pcamp: Performance comparison of machine learning packages on the edges," in *{USENIX} Workshop on Hot Topics in Edge Computing (HotEdge 18)*, 2018.
- [111] B. I. Team, "Skripal Suspect Boshirov Identified as GRU Colonel Anatoliy Chepiga," 2018.
- [112] —, "Full Report: Skripal Poisoning Suspect Dr Alexander Mishkin Hero of Russia," 2018.
- [113] M. Farrell, "Assassination and Poisoning," in *Criminology of Poisoning Contexts*. Springer, 2020, pp. 69–92.

- [114] C. Levett, F. Sheehy, P. Guest, and L. Smears, "Visual guide: how the novichok suspects made their way to Salisbury," <https://www.theguardian.com/uk-news/2018/sep/05/novichok-poisoning-what-we-know-so-far>, 2018.
- [115] M. Guri and D. Bykhovsky, "air-jumper: Covert air-gap exfiltration/infiltration via security cameras & infrared (ir)," *Computers & Security*, vol. 82, pp. 15–29, 2019.
- [116] A. Cui, M. Costello, and S. Stolfo, "When firmware modifications attack: A case study of embedded exploitation," 2013.
- [117] A. Costin and J. Zaddach, "IoT malware: Comprehensive survey, analysis framework and case studies," *BlackHat USA*, 2018.

APPENDIX A

OUR SYSTEM APPLIED TO A REAL-LIFE THIRD-PARTY EXPERIMENT ON CCTV AND PRIVACY BY PASLEY [2]

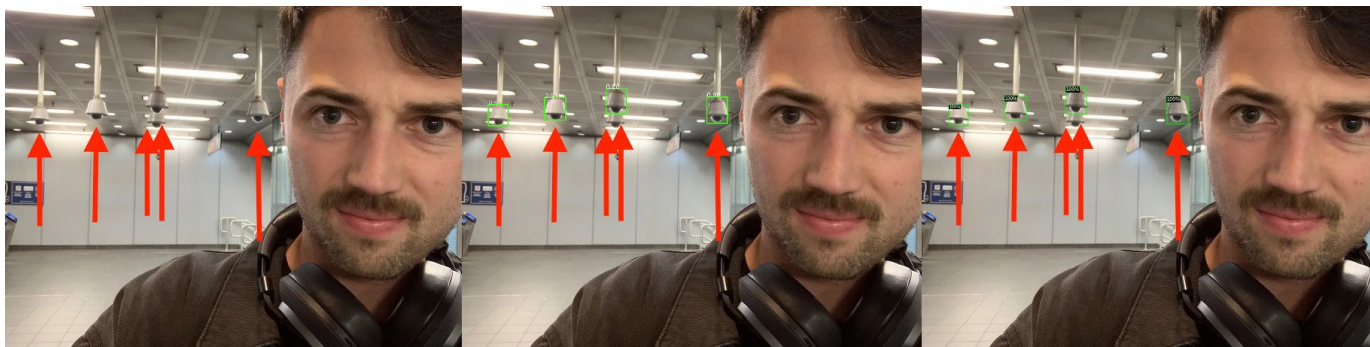


Fig. 14. Visual results (left to right): Original image (Ground Truth) - 5 TP; ATSS X-101 - 4 TP, 1 FN; TridentNet R-101 - 4 TP, 1 FN

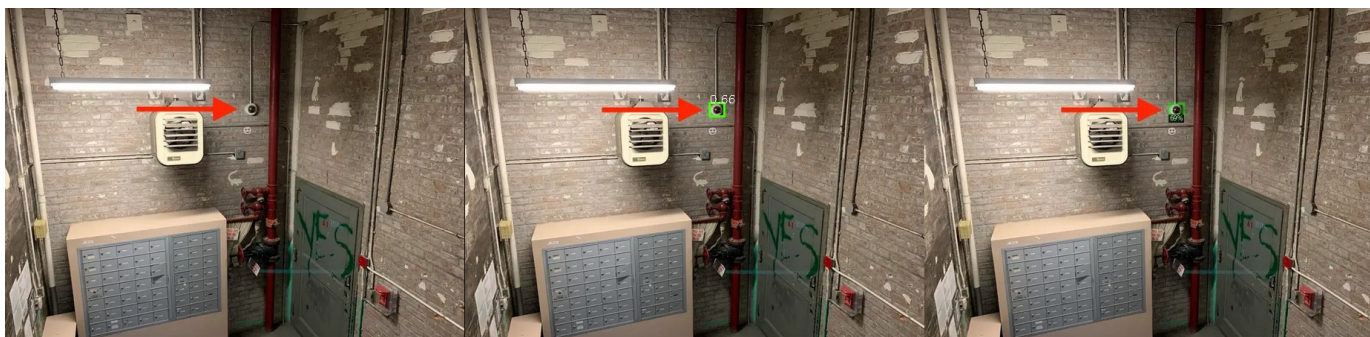


Fig. 15. Visual results (left to right): Original image (Ground Truth) - 1 TP; ATSS X-101 - 1 TP; TridentNet R-101 - 1 TP



Fig. 16. Visual results (left to right): Original image (Ground Truth) - 1 TP; ATSS X-101 - 1 TP; TridentNet R-101 - 1 FN



Fig. 17. Visual results (left to right): Original image (Ground Truth) - 1 TP; ATSS X-101 - 1 TP; TridentNet R-101 - 1 TP, 1 FP



Fig. 18. Visual results (left to right): Original image (Ground Truth) - 2 TP; ATSS X-101 - 2 TP; TridentNet R-101 - 2 TP

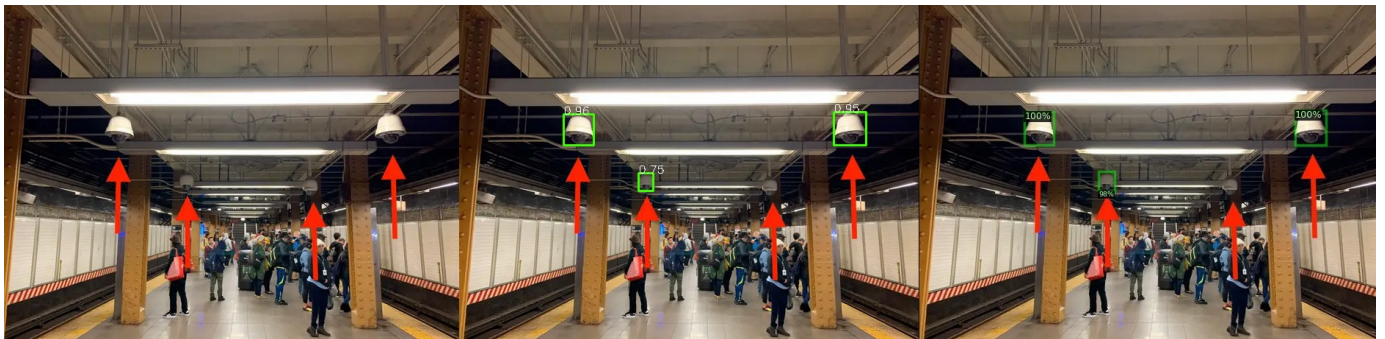


Fig. 19. Visual results (left to right): Original image (Ground Truth) - 4 TP; ATSS X-101 - 3 TP, 1 FN; TridentNet R-101 - 3 TP, 1 FN

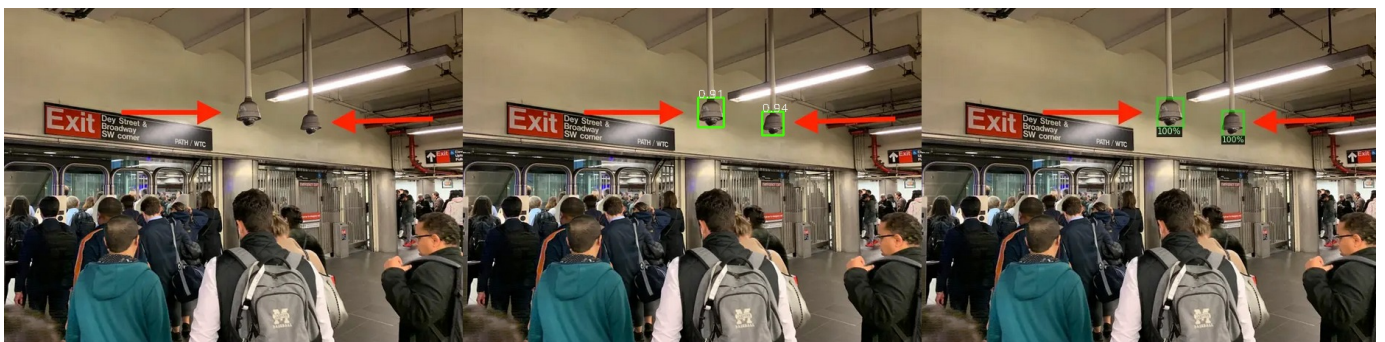


Fig. 20. Visual results (left to right): Original image (Ground Truth) - 2 TP; ATSS X-101 - 2 TP; TridentNet R-101 - 2 TP



Fig. 21. Visual results (left to right): Original image (Ground Truth) - 5 TP; ATSS X-101 - 5 TP; TridentNet R-101 - 4 TP, 1 FN



Fig. 22. Visual results (left to right): Original image (Ground Truth) - 1 TP; ATSS X-101 - 1 TP; TridentNet R-101 - 1 TP



Fig. 23. Visual results (left to right): Original image (Ground Truth) - 1 TP; ATSS X-101 - 1 FN; TridentNet R-101 - 1 TP. NOTE: When the original author's red arrow is removed, it proved quite challenging for humans to quickly detect the CCTV camera as it "hides" behind a corner and blends into the dark background.